# A THEORETICAL ANALYSIS OF PROGRESSIVE AND RETROGRESSIVE FAILURE IN DISCONTINUOUS ROCK MASSES SUBJECTED TO 'IN-SITU' SHEAR

## 'Yerinde' Makaslamaya Tabi Tutulan Süreksiz Kayaç Kütlelerinde İleri ve Geri Yenilmenin Teorik Analizi

*Kadri Erçin Kasapoğlu*
Hacettepe Üniversitesi Yer Bilimleri Enstitüsü

ABSTRACT. — *This paper presents a study of shear deformation which includes a theoretical approach to progressive and retrogressive failure, involving discontinuous and elastic-elatoplastic finite element method. It has been concluded that choice of boundary conditions exertd an important control on failure mechanism. Under certain boundary conditions, the ultimate failure of the test block is a consequence of multiple fracture mode. 'In-situ' shear tests on geological materials should be interpreted in more sophisticated terms; i.e., as a consequence of variable combined stress state, involving inhomogeneous stress field, one or several of principal stresses being tensile; extensive stress reorientation; and multiple crack propagation. The theoretical approach to the mechanism of shear deformation. The theoretical approach to the mechanism of shear deformation and failure characteristics of 'ın-situ' shear tests, utilizing finite element method, appears to be a valid approach for prediction of certain experimental results.*

ÖZ. — *Bu yazıda takdim edilen makaslama deformasyonu çalışması, süreksiz ve elâstik-elastoplastik sonlu elementler metodu ile, ileri ve geri yenilmenin teorik analizini kapsamaktadır. Bu çalışmadan çıkarılan sonuçlara göre, kenar yükleme şartlarının seçiminin yenilme mekanizmasının kontrolü yönünden çok önemli etkileri vardır; belirli kenar yükleme şartları altında, deneme blokunun en son yenilmesi birden fazla kırılma şeklinin bir neticesidir. Jeolojik materyaller üzerinde yapılan 'yerinde' makaslama denemeleri, daha değişik bir terminoloji ile, bir veya birkaç asal gerilmenin tansiyon şeklinde, olduğu, homojen olmayan bir gerilme alanı, yaygın bir gerilme reoriyantasyonu ve birden fazla çatlak ilerlemesi gibi değişebilen birleşik gerilme hallerinin bir neticesi olarak değerlendirilmeli ve açıklanmalıdır. 'Yerinde' makaslama denemelerindeki makaslama deformasyonunun ve yenilme mekanizmasının, sonlu elementler metodu ile yapılacak teorik analizleri ile bazı deneysel neticeleri önceden belirliyebilmek mümkündür.*

## INTRODUCTION

Direct tests in the laboratory and in 'in-situ' field conditions are important sources of information on strength parameters for soil and rock materials, for both geologic and engineering purposes.

Despite this widespread usage, the physics of deformation involved in these tests are not well understood, and as a result important misinterpretations of the data resulting from sheartesting are possible. One purpose of this work has been, in fact, to obtain some general information on actual mechanism of shear deformation and shear sailure in both laboratory and 'in-situ' shear tests, and shed light upon some of these difficulties, in particular the development of progressive failure in isotropic and anisotropic non-linear materials as a function of the method of application of boundary forces.

Under conditions in which all stresses are compressive and normals stresses on all discontinuities are high, it is realistic to treat the roch system as an elastic continuum. However, the possibility of development of the tensile stresses at the base of the block is considered to be extremely important for understanding of the mechanism of deformation and failure in 'in-situ' shear tests. Any displacement within the rock mass may change the relative position of the rock "block" and result in high localized stresses on them, which may cause individual localized failures. These fadlures may be of tensile, indirect tensile, or shear mode type. The stresses in the rock system may redistribute themselves in a characteristic fashion after localized failures.

Progressive type failure is very common in many soil and rock materials. Understanding of the mechanism of this type of failure is very important; yet the conditions underwhich it may occur are poorly understood.

## ANALYSIS TECHNIQUES

The finite element method (FEM) has been employed to analyze stresses and strains in plane-strain shear block model. The concept utilized here, as described by Wang and Voight (1969). involves the ordinary finite element partitioning of a solid model into a discrete number of two-dimensional elements with "dual nodal points" used along prescribed planes of discontinuity. A Coulomb-Navier representation with a tension cut-off hasbeen uti-

lized. Progressive failure in the potential shear zone (i.e., a plane of discontinuity at the base of the shear block) has been considered.

Dahl's (1969) finite element code with suitable modifications has also been used for the elastic-elastoplastic analysis; the material is gisumed elastic- perfectly plastic and analysis has been based on elastic-elastoplastic idealization. Formulation of the problem is in terms of incremental theory of plasticity where by constitutive nonlinearity in the post-yield region is analyzed in a number of increments (Dahl, 1969; Dahl and Voight, 1969; Voight and Dahl, 1970). Each increment is independent ; total stresses and strains from the previous increment are added to the incremental stresses and strains of the present increment in order to compute total stresses and strains of the presents increment,

## MODEL FORMULATION

Two basic computer models, labeled M1 and M2 Figures 1, 2 were developed for the theoretical analysis by finite elemant techniques and used during the course of this investigation.

M1: a model of an 'in-situ' shear bloch with three internal discontinuties, labeled Dl, D2 and DS; where Dl concides with the hypothetical shear plane at the base of the block ; and D2 and D3 coincide with potential tension fractures predicted from experimental analysis. This is the model most commonly used for the elastic analysis in ipajor part of this study.

M2: a model of an 'in-situ' shear block with no discontinuity. This model was principally employed for the elastic-elastoplastic analysis.

The two-dimensional idealization was assumed to provide an adequate approximation to prototype conditions.

The analysis has been limited to one particular rock, Berea sandstone; the mechanical behavior of this rock was well suited to the requirements of this study; data on its physical properties was unusually complete and was available to the author (Table 1). The material constants for the elastic, homogeneous and isotropic continuum were E = 1.1 X $10^6$ psi., and $v$ = 0.2. The material constants for the transversely isotropic continuum were as given below :

$E_n$ = 1.1 X $10^6$ psi $\quad$ $E_t$ = 0.6 X $10^6$ psi.

$v_n$ = 0.2 $\quad$ $v_t$ = 0.13

G = 0.46 X $10^6$ psi.

## BOUNDARY CONDITIONS

Eight different ways of loading the shear block model, in terms of various force and displacement boundary conditions, were considered (Figures 3) ; these conditions are described as follows.

L1: Uniformly distributed load parallel to the base of the block.

L2: Uniformly distributed load parallel to the base of the block; and uniformly distributed load perpendicular to the base of the block.

L3: Uniform displacement of the left-hand side of the block parallel to its base.

L4: Uniform displacement of the left-hand side of the block parallel to its base ; and uniformly distributed load perpendicular to the base of the block.

L5: Uniformly distributed load parallel to the base of the block as concentrated at the lower third of the block.

L6: Uniformly distributed load parallel to the base of the block as concentrated at the lower third of the block; and uniformly distributed load perpendicular to the base of the block.

L7: Uniformly distributed load inclined to the base of the block at an angle of 20°.

L8: Uniformly distributed load inclined to the base of the block at an angle of 20° ; and uniformly distributed load perpendicular to the base of the block.

TABLE 1

**Nominal Valu of of the Physical Properties of Berea Sandstone (After Khair, 1971)**

| **Physical Property** | **Value** |
|---|---|
| Unconfined Compressive Strength | 9.000 psi. |
| Unconfined Tensile Strength | 300 psi. |
| " Shear " | 1.400psi. |
| Young's Modulus in Compression | $1.15X10^6$ psi. |
| Young's Modulus in Tension | $0.58X10^6$ psi. |
| Poisson's Ratio in Compression | 0.2 |
| Poisson's Ratio in Tension | 0.1 |
| Independent Shear Modulus | $0.46X10^6$ psi. |

## RESULTS AND DISCUSSION

The results for the elastic continuum, discontinuum, and elastic-elastoplastic solutions are grouped and considered in three separate sections.

### 1. Elastic Continuum Solutions

Results of plane strain FEM analyses using model M1 and assuming an elastic, homogeneous and «either isotropic or transversely isotropic continuum are presented herein, for various boundary conditions in terms of:

*Principal stress distribution:* All analytical solutions, in terms of direction and magnitude of major and minor principal stresses, were plotted by computerized (CalComp) plotter at the centroid of each triangular element A typical isotropic solution data for the boundary condition L-4 is presented in Figure 4. Direction and magnitude of the major and minor principal stresses are inhomogeneously distributed throughout the rock mass, with significant variations across the hypothetical shear plane at the base of he block and significant stress concentrations at the corners. The zone of principal stresses in tension is most extensive for purely edge loaded models (L-1,2,3,5,7) being somewhat more suppressed for the displacement boundary condition (L-3) and for concentrated loading (L-5). There are significant changes in the principal stress directions as function of boundary conditions; in all cases the steepness of the principal compression trajectory is enhanced by application of normal force to the shear block; the most extreme examples are perhaps L3, and L-4 where application of normal force was sufficent to alter a predominantly sub-horizontal compression axis to a predominantly subvertical orientation.

*Distribution of strains and stresses at the base of the block:* Both strains and stresses at the base of the block are distributed nonuniformly for all boundary conditions. In general, both normal and tangential strains, as well as the normal and tangential stresses have tensile (reckoned positive) values in the left-hand part of the base of the block for L- 1, 3, 5, 7; ie., for conditions without vertical confinement. For the boundary conditions L-2 and L-8 the extensile strains and tensile stresses remain, and even then only for the tangential components. Figures 5 and 6 show the distribution of strain and stresses at the base of the block for the bound-

ary conditions L-3 and L-4. For the boundary conditions L-4 and L-6, all the strains and stresses are compressive, i.e., no extensile strains or tensile stresses occur at the base of the block. This situation is considered important because this is the only situation in which failure of the block could initiate wholly as a consequence of shearing. However, even for these models, tensile regions exist may be mechanical significance in direct shear testing. For example, Figure 7 shows the distribution of the strains and stresses along the inclined discontinuity D3 (see Figure 1) for the L-4 boundary condition at the incipient yield. Initial yielding occurs in the tension mode at the free boundary of discontinuity D3 as a consequence of high tensile stress concentration at the corner.

*Dependence of tensile zone of normal force:* Figure 8 shows the progressive development of a tensile zone en the block with respect to various ratios of applied normal force to applied tangential (edge) force. The area of the tensile zone increases as the ratio of normal to tangential force (R) decreases. There is no tensile zone developed at the base of the block for R = $^{\infty}$ (i.e., $F_y$ = O) ; conversely the tensile zone is the largest for R = O (i.e., $F_x$ = O).

*Maximum shear stress contours:* Contours of the maximum shear stresses developed in the shear block under various boundary conditions were plotted in the neighbourhood of the block base. For most boundary conditions, concentration of the maximum shear stresses occurs near the corners of the base of the block, but not necessarily the pilane of the rock block base. This fact, also reported by Ruiz et al, 1968; possibly explains the occurrence of shear failure surfaces out of the plane of the block base on a number of tests reported by various investigators (e.g., Evdokimov and Sapegin, 1970). Concentration of the maximum shear stress contours around the right-hand corner of the block base also points out the effect of rotational deformation of the shear block on faillure mechanism. The boundary conditions L-3 and L-4 are the only conditions underwhich this effect is minimized due to minimized rotation of the block. Figure 9 shows the maximum shear stress contours in the neighbourhood of the block base for the boundary condition L-4

*Displacement fileld and distortion of the block:* The total displacements of the nodal points were also plotted on a CalComp plotter. Figure 10 and 11 show the elastic displacement fields for the boundary conditions L-3 and L-4. Distortion characteristics of

the block corresponding to the boundary displacement field for L-3 and L-4 are shown in Figure 12. These results show that type of deformation in the block basically depends upon the nature of the appilied boundary conditions.

## 2. Discontinuum Solutions

The results presented in the previous section represent loading conditions associated ith incipient initial failure. Any further increase in that critical tangential load causes (at least local) failure along any one of hree discontinuities D1, D2, D3 (see Figure 1), in either a slip or separation mode.

*Mode of deformation*: The theoretical results are of interest, clearly showing the dependence of failure mode on the boundary conditions. Al boundary conditions, except for L-4, resulted in initial yielding of the block at the first node of the discontinuity D1, in the form of dual node separation; failure propagated along that discontinuity in the separation mode until complete failure occured in the form of separation of aill dual nodes on D1. For boundary condition L-4. however, yielding of the block initiated in the separation mode at the top the discontinuity D3 ; failure propagated diagonally along D3 until the last dual nodes on D3 are separated (Figure 13). This is considered to be the termination of the "first stage" of faillure. Further (loading after the complete opening of D3, produced the initiation of the "second stage" of failure, this time at the base of the block at the first dual nodes of D1 in the "slip" mode (i.e., shear). This second sage of failure progressed towards the center of the block in the "slip" mode betweeen subsequent dual nodes. At the time the second stage of failure reached to about one-sixth of the total length of D1 from the left-hand corner, a "third stage" of failure of the block was initiated on D1 at the opposite corner, and retrogressed towards the center of the block in the "slip" mode. Complete rupture at tba base of the block occured when the progressive and retrogressive failure surfaces met on Dl in the middle of the block base (Figure 14). The progressive and retrogressive failure series with associated displacement fields and principal strfess distributions are summarized in Figures 15, 16 and 17, respectively.

*Mechanism of failure:* In most cases concentration of tensile stresses occured around the left-hand corner of the shear block. Initial failure thus occurred at this corner in form of a tensile crack which opened and propagated diagonally along the discontinuity D3. Separation along D3 releases tensile stresses originally develop ed and thus causes a redistribution of strains and stresses along the base of the block (Figure 18) ; this redistribution is responsible for subsequent failaure along D1, predominantly in the "slip" (shear) mode. A temporary cessation of crack propagation, and the inception of a "third stage' ' of failure associated with retrogressive stlip at the opposite corner, can also be explained in terms of subsequent stress redistribution, which finally results in critically high shear stress concentration at he lower lefthand corner of the shear block.

*Peak and residual strength and progressive failure:* Two series of experiments were conducted; in the first series, constant strength parameters (i.e., experimentally determined peak values for CF, SS and TS) (Table 2) were assigned to D1 and were maintained as the edge displacements were applied in successive increments. The total edge displacement required in order to cause "slip" (shear failure) at each successive nodal point along D1 were determined (Figure 19). In the second series, peak strength parameters were initially prescribed, but not necessarily maintained. A new set of strength parameter (i.e., exprimentally determined residual value for CF; Zero for SS, and for TS) were subsequenttly assigned to the each posint on D1 if a minimum horizontal displacement between dual nodes reached to a specified critical value (i.e., uy = $1.0+10^{-5}$ in.) in the previous loading increment; the original peak strngeth values are retained for points which had either not yet failed in the "slip" mode, or which had not undergone sufficient "slip". The applied edge displacements required to cause shear failure were determined for each successive point. Results obtained for this series are also summarized in Figure 19. The shear strength failure envelopes predicted from these two series of computer experiments are plotted together which the "intrinsic" peak and residual strength failure envelopes, drawn on the basis of the fundamental values of SS and CF (Figure 20). The results are of interest, clearly showing the significant differences between the fundamental values of SS and CF (Figure 20). The results are of interest, clearly showing the significant differences between the fundamental values of SS and

CF, and the predictide values SS', and CF'; and the effect of residual values of $TS^R$, $SS^R$ and $CF^R$ on the shear strength characteristics of the rock.

TABLE 2

**Fundamental Values of CF, SS. and TS Assumed Along the Discontinuities D1, D2, D3.**

| Discontinuity | CF | SS | TS |
|---|---|---|---|
| D1 | 0,65* | 1200* psi | 300 psi |
| D2 | 0.975 | 1800 psi | 450 psi |
| D3 | 0.975 | 1800 psi | 450 psi |
| | 1.30** | 2400** psi | 583psi**psi |

* Values determined by experiments in the direction parallel to the bedding.

** Values determined by experiments in the direction normal to the bedding.

## 3. Elastic-Elastoplastic Solutions

Elastic-elastoplastic analyses of the direct shear problem were limited to the boundary conditions L-2, L-3 and L-4; model M2 (see Figure 2) was employed. Distribution of the major and minor principal stresses in the plastic state of the block, corresponding plastic displacement fields and the progressive yield zones for tye above boundary conditions were considered; as were assumption of both linear (Colomb) and non-linear (Torre) yield criteria. The elastic and strength properties used for the elastic-elastoplastic solutions are given in Table 3.

*Distribution of principal stresses:* Nature of principal stresses (i. e., either being tensile or compressive), in the plastic state of the block, were found to depend primarily upon the boundary conditions. Neither transverse isotropy nor non-linearity of the yield functions employed showed any significant effect on the direction and the nature of the principal stresses when compared with the isotropic and linear analysis. Distribution of the principal stresses in the plastic state of the block, under the boundary condition L4, is shown in Figure 21. Location of the principal stresses in tension, and their direction around the lower left-hand corner of the block support the previous discussion on the mode of initial failure of the shear block.

*Displacement fields:* For the similar boundary conditions, neither, non-linearity of the failure criteria used, nor the transverse isotopy assumed showed any significant effect on the nature of the displacements. The differences between the boundary conditions is primarily one of variations in slope of the displacement vectors (Figures 22 and 23).

*Development of plastic zones:* The location of the zone of plastic elements appears to be affected in large measure by the development of tensile stresses; it is not extensively developed in regions of large compressive stress. Both the point of initiation and the direction of propagation of the plastic elements appears to be in good agreement with the pint of initiation and the direction of propagation of (extensional) yielding. When applied edge displacement is further increased, the progression of the plastic zone continues along the base of the shear block still in the form of (extensional) yielding (Figures 24 and 25). Plastic yielding occurs along the upper boundary of the shear block seems to be the result of tensile stresses which develop in that region due to the nature of the applied boundary condition, L-4. These tensile stresses apear to be perpendicular to the left-hand boundary of the shear block where edge displacements are applied to the block. This is, however, physically and unrealistic situation; this type of failure probably will not occur under actual test conditions.

TABLE 3

**The Elastic and Strength Properties Used For Elastic-Elastoplastic Solutions.**

| **Elastic properties:** | **Isotropie Case** | **Transversely Isotropic Case** |
|---|---|---|
| $E_1$ | 1.1X10$^6$psi | 1.1X10$^6$psi |
| $E_2$ | 1.1X 10$^6$psi | 0.58X10$^6$psi |
| $v_1$ | 0.2 | 0.2 |
| $v_2$ | 0.2 | 0.1 |
| G | 0.46X10$^6$psi | 0.46X10$^6$psi |
| **Strength Properties:** | | |
| $CS_n$ | 9000 psi | 10000 psi |
| $CS_t$ | 9000 psi | 7000 psi |
| $TS_n$ | 300 psi | 500 psi |
| $TS_t$ | 300 psi | 200 psi |
| SS | 1400 psi | 1400 psi |

## SUMMARY

This paper presents a study of progressive shear deformation which involved a computer experimentation employing elastic continuum, discontinuum and elastic-elastoplastic finite element method. Two basic computer shear block models were developed for this purpose. Two-dimensional plane-strain idealization was assumed. Eight different methods of loading the shear block model were considered. A discussion of failure mechanism, in terms of progressive and multiple modes of failure, was introduced.


## CONCLUSIONS

Results of the preceeding analyses led to the following general conclusions: Choice of boundary conditions exerts an important control on failure mechanism.

Tensile zones always developed within test block in response to applied shear force are of mechanical importance : Local failure which occurs, in separation mode, in these tensile zones leads to progressive failure. Under certain boundary conditions, the ultimate failure of the test block is a consequence of multiple fracture modes.

Mechanical behavior and strength of an 'in-situ' shear block can not be adequately explained solely in terms of some fundamental shear strength parameters only. Importance of rock mass tensile strength which is generally very low, and pre-existing discontinuities, which offer little tesile resistance, should not be overlooked in 'in-situ' shear experiments, in asmuchas they extent important control on force-displacement relationship measured by such tests.

'In-situ' shear tests on geological materials should be interpreted in more sophisticated terms, i.e., as a consequence of variable stress states, involving inhomogeneous stress field, one or several of principal stresses being tensile; extensive stress reorientation; and multiple crack propagation.

Uniform edge-displacement boundary condition produces the most consistent theoretical results; hence may be suggested as a standard method of application of shear force to the test block both in 'in-situ' and laboratory shear experiments.

Discontinuum solutions, utilizing discontinuous model; allow prediction of localized failures and analysis of progressive nature of failure mechanism. Elastic-elastoplastic solutions, on the other hand, appear to be more suitable for analysis of progressive de-

velopment of yield zones in areas around the points of high stress concentrations.

**ÖZET**

'Yerinde' makaslama denemelerinde deformasyon ve yenilme mekanizmasının saptanması amacı ile yapılan bu çalışmada, sorun önce teorik yönden ele alınmış ve tipik bir 'yerinde' makaslama blokunun detaylı bir kompüter (matematiksel) modeli geliştirilmiştir. Bu model üzerinde, düzlem-deformasyon şartları varsayılarak, sonlu elementler metodu ile, değişik kenar yükleme şartları altında gerilim ve deformasyon analizleri yapılmıştır.

Teorik analiz sonuçları, deformasyon modunun kenar yükleme şartlarına bağlı olduğunu açık bir şekilde ortaya koymuş olması bakımından ilginçtir. L-4 kenar yükleme hali dışında, diğer bütün yükleme şartları altında, makaslama blokunun ilk yenilmesi D1 süreksizliği üzerinde, sol uçtaki ilk noktada, blokun tabandan ayrılması (tansiyon yenilmesi) şeklinde oluşmaktadır. Uygulanan makaslama yükünün sürekli olarak arttırılması halinde, blokun ilk yenilmesi ile oluşan tansiyon çatlağı blok tabanı (D1 süreksizliği) boyunca sağa doğru ilerlemekte; blokun son yenilmesi ise, D1 süreksizliği boyunca makaslama blokunun tabandan tamamen ayrılması şeklinde oluşmaktadır. D-4 kenar yükleme şartı altında, makaslama blokunun ilk yenilmesi bu defa D3 süreksizliğinin üst uç kısmında, yine 'ayrılma' (tansiyon yenilmesi) şeklinde oluşmakta ve meydana gelen tansiyon çatlağı D3 boyunca ilerlemektedir. Makaslama blokunun D3 süreksizliği boyunca tamamen ayrılmış hali ve o andaki dış deformasyonu Şekil 13 de gösterilmiştir. Yenilmenin 'ilk evre' si olarak tanımlanan bu durumdan sonra, uygulanan makaslama yükünün sürekli olarak arttırtılması halinde, yenilmenin 'ikinci evre'si blok tabanı boyunca, D1 süreksizliğinin sol ucunda 'kayma' (makaslama yenilmesi) şeklinde oluşmakta ve sağ uca doğru ilerlemektedir. Bu şekilde oluşan makaslama çatlağı, D1 uzunluğunun henüz altıda biri kadar ilerlemiş iken, yenilmenin 'üçüncü evre' si makaslama blokunun sağ alt köşesinde, D1 üzerinde yine bir 'kayma' (makaslama yenilmesi) şeklinde oluşmaktadır. Sağ köşeden geriye (sola) doğru ilerleyen bu makaslama çatlağı, blok tabanının orta kısmında, sol köşeden sağa doğru ilerlemekte olan 'ikinci evre' çatlağı ile birleşerek deneme blokunun 'tüm yenilme' sini oluşturmaktadır.

Gerilim analizlerinden elde edilen sonuçlara göre, çoğunlukla, tansiyon gerilimi yoğunlaşması makaslama blokunun sol alt köşesinde oluşmaktadır. Yenilmenin 'ilk evre' si sırasında D3 bo-

yunca oluşan tansiyon çatlağının açılması, makaslama blokunun sol alt köşesinde yoğunlaşmış olan tansiyon gerilimlerinin boşalmasına sebep olmaktadır. Bunun sonucu olarak da, blok içerisinde yeniden bir gerilim dağılımı oluşmakta ve bu da, D1 süreksizliği boyunca, yenilmenin ikinci ve üçüncü evreleri sırasında oluşan 'kayma' şeklindeki yenilmelere sebep olmaktadır. İkinci evre sırasında makaslama blokunun sol alt köşesinde oluşan makaslama çatlağının D1 boyunca ilerlemesinin geçici olarak durması veya yavaşlaması; ve karşıt köşede, yenilemenin üçüncü evresinin 'kayma' (makaslama yenilmesi) şeklinde oluşması da yine, birinci ve ikinci evreler sonunda, her defasında yeniden oluşan gerilim dağılımının makaslama blokunun sağ alt köşesinde sebep olduğu büyük makaslama gerilimi yoğunlaşmasının bir sonucu olarak açıklanabilir.

Bu analizler sırasında, deneme bloku içerisinde ve süreksizlik düzlemleri boyunca, tansiyon çatlakları şeklinde oluşan lokal yenilmelerin deneme blokunun son yenilmesi üzerinde, mekanik yönden çok önemli bir rol oynadıkları saptanmıştır. Bu nedenle, gerek 'yerinde' gerek laboratuarda yapılacak makaslama denemelerinde, kayaçların çok düşük olduğu bilinen çekme (tansiyon) dayanımlarının ve kayaç yapısında bulunabilecek süreksizlik düzlemlerinin özellikle dikkate alınması gerekir.

## REFERENCES

Dahl, D. and Voight, B., 1969 "Isotropie and anisotropic plastic yield associated with cylindrical underground excavations" — Proc. Int. Symp. on Large Permanent Underground Openings, Oslo.

Evdokimov, P,. D. and Sapegin, D. D., 1970 "A large scale field shear test on rock" — Proc. 2nd. Conf. Int. Soc. Rock Mech., Belgrade, v. 2 pap 3-17.

Khair, A. W. 1971 "A study of mechanical properties of Berea sandstone for use in the A.G.A. large model studies" — The Pennsylvania State University Internal Report RML-IR/71-20.

Ruiz, M. D., Camargo, F. P. and Nieble, C.M., 1968 "Some considerations regarding the shear strength of rock masses" — Int. Symp., on Rock Mech., Madrid, 159-161.

Voight, B., 1969 "Numerical continuum approaches to analysis of non-linear rock deformation" — Conf. on Research in Tectonics, Hamilton, Ontario.

Wang, Y. J. and Voight, B., 1969 "A discrete element stress analysis model for discontinuous materials" — Proc. Int. Symp. on Large Permanent Underground Openings, Oslo.

## NOMENCLATURE

The following defines the major symbols used in this text.

| | |
|---|---|
| E | Young's modulus |
| $E_n$ | Young's modulus an the direction normal to the discontinuity D1 |
| $E_t$ | Young's modulus in the direction parallel to the discontinuity D1 |
| *v* | Poisson's ratio |
| $v_n$ | Poisson's ratio in the direction normal to the discontinuity D1 |
| $v_t$ | Poisson's ratio in the direction parallel to the discontinuity D1 |
| G | Independent elastic shear modulus |
| CF | Coefficient of friction |
| CS | Compressive strength |
| $CS_n$ | Compressive strength in the direction normal to the discontinuity D1 |
| $CS_t$ | Compressive strength in the direction parallel to the discontinuity D1 |
| TS | Tensile strength |
| $TS_n$ | Tensile strength in the direction normal to the discontinuity D1 |
| $TS_t$ | Tensile strength in the direction parallel to the discontinuity D1 |
| SS | Shear strength |
| $F_x$ | Total boundary force applied in x-directicn |
| $F_y$ | Total boundary force applied in y-direction |
| $F_{xy}$ | Total boundary force applied in x-y plane |
| $U_x$ | Total edge displacement in x-direetion |
| $U_y$ | Total edge displacement in y-direction |
| σ | Stress |
| $\sigma_x$ | Stress in x-direction |
| $\sigma_y$ | Stress in y-direction |
| $\tau_{xy}$ | Shear stress |
| $\tau_{max}$ | Maximum shear stress |
| ε | Strain |
| $\varepsilon_x$ | Strain in x-direction |
| $\varepsilon_y$ | Strain in y-direction |
| $\varepsilon_{xy}$ | Shear strain |

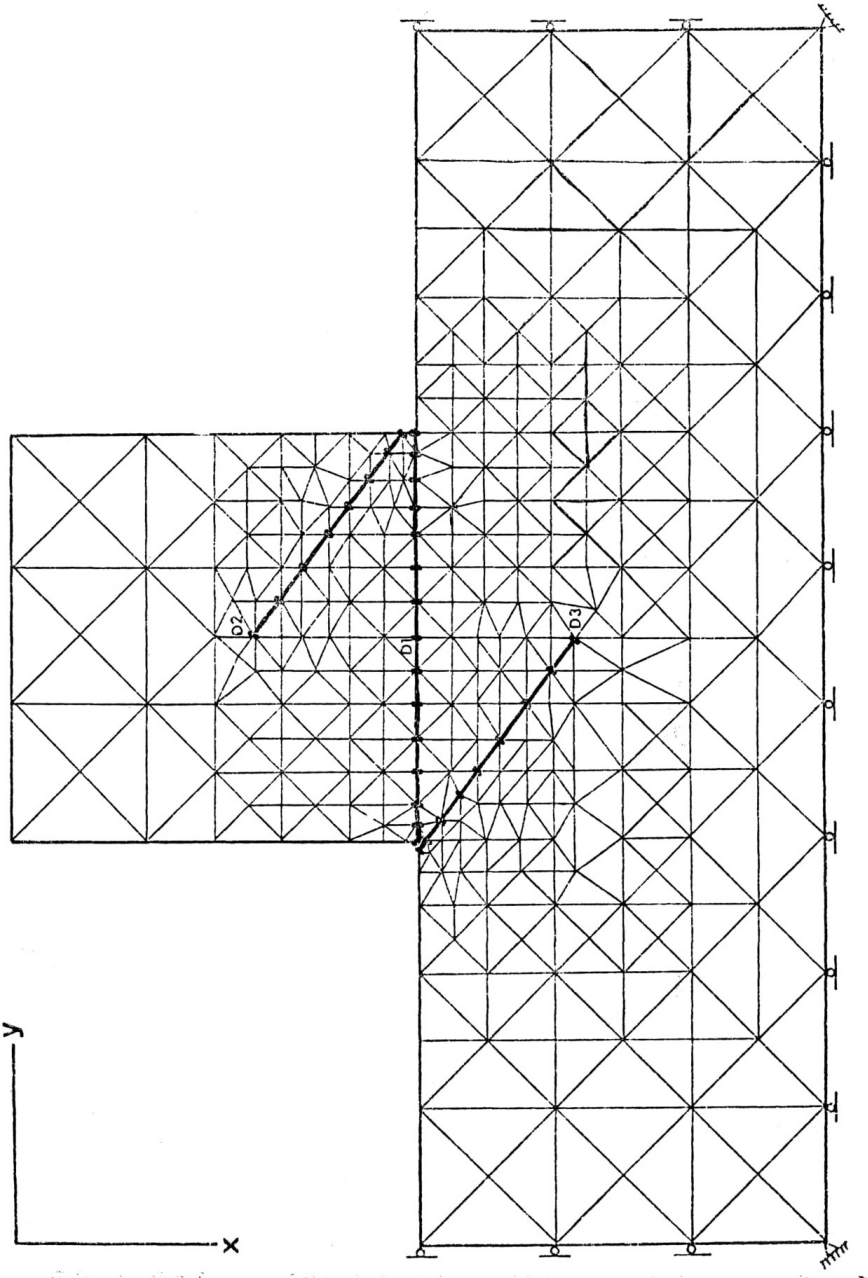


**Figure 1. Finite element idealization of 'in-situ' shear block model M. 1**

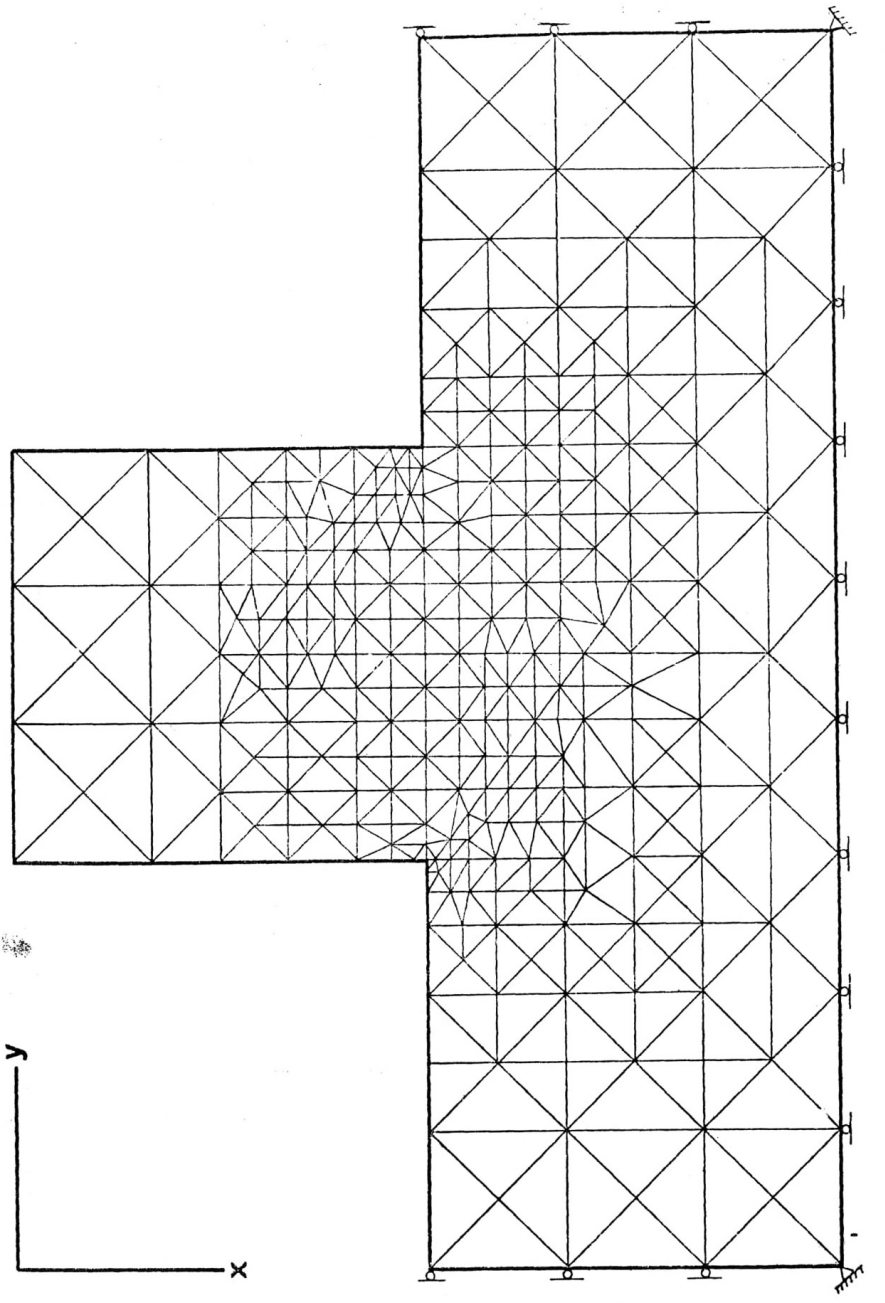


**Figure 2. Finite element idealization of 'in-situ' shear block model M2.**

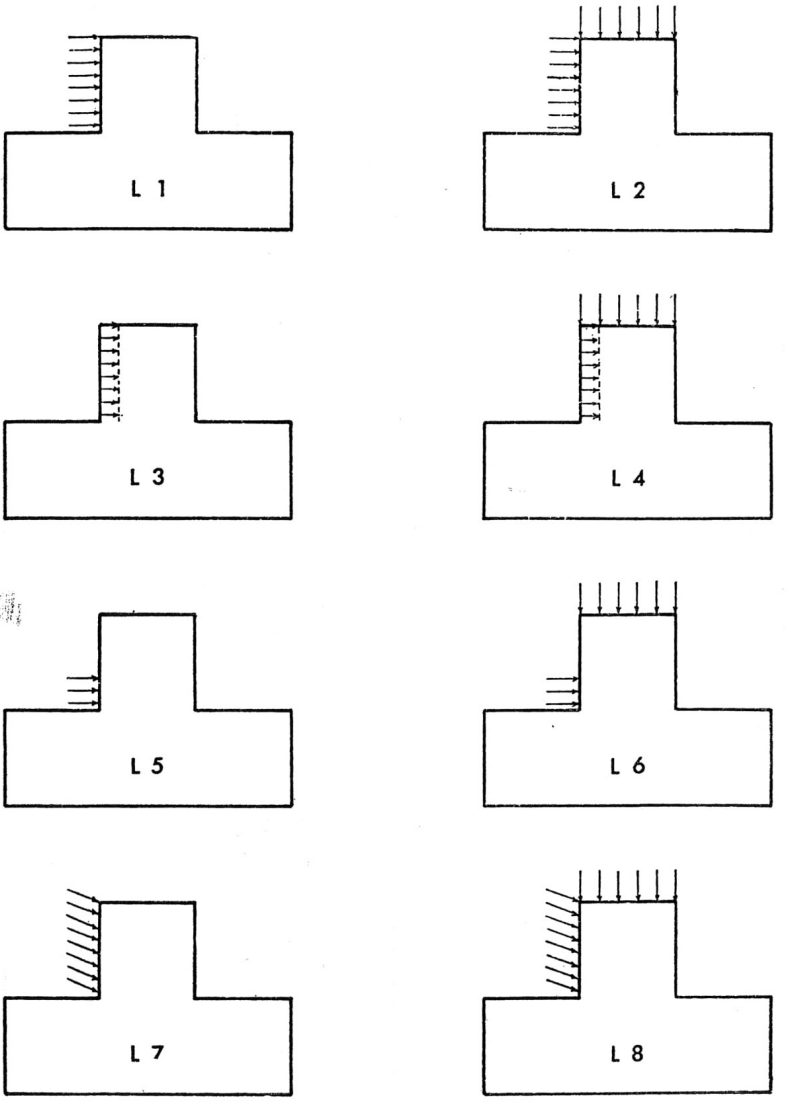


**Figure 3. Boundary conditions.**

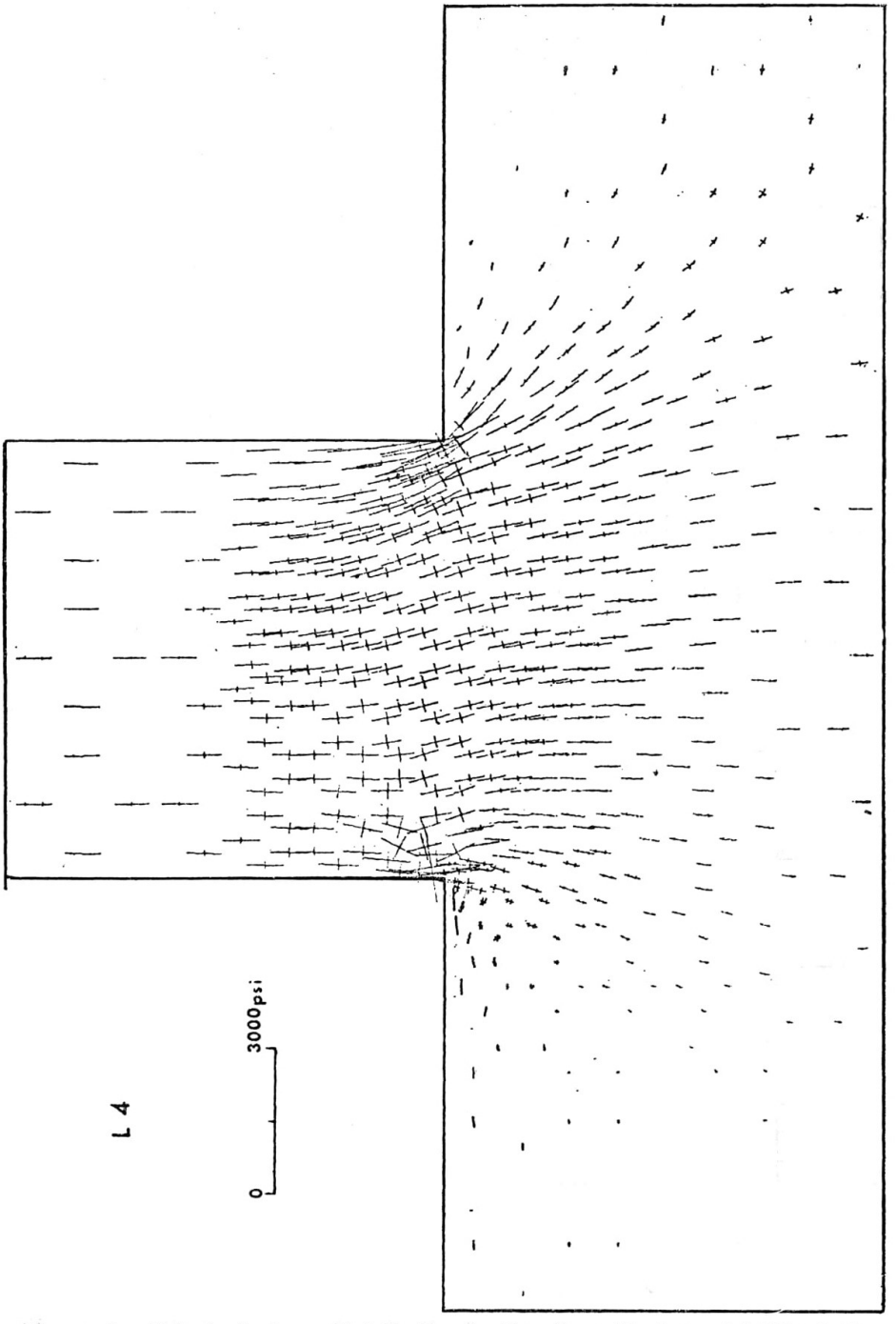


**Figure 4. Principal stress distribution in the shear block model M1 at the point of incipient yield.**

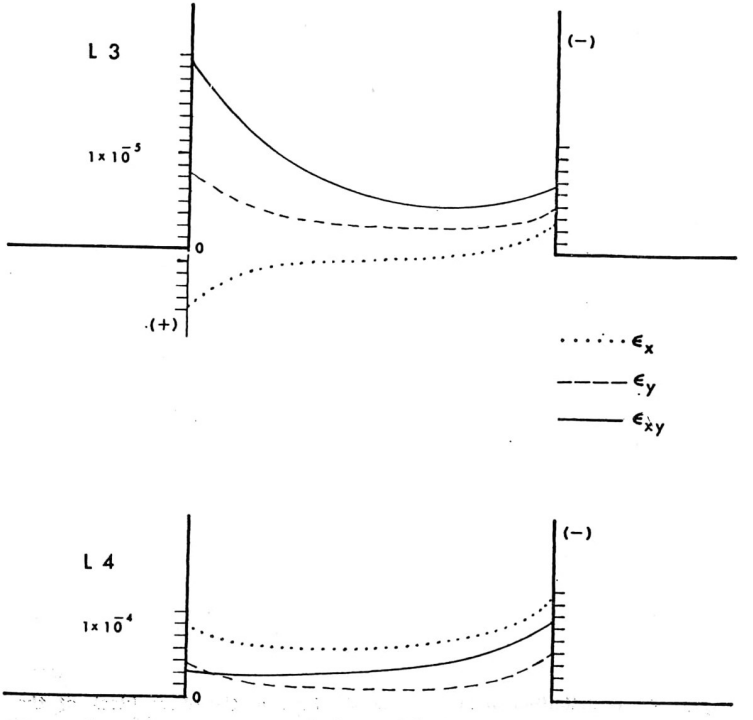


**Figure 5. Distribution of strains at the base of the shear block at the incipient yield.**

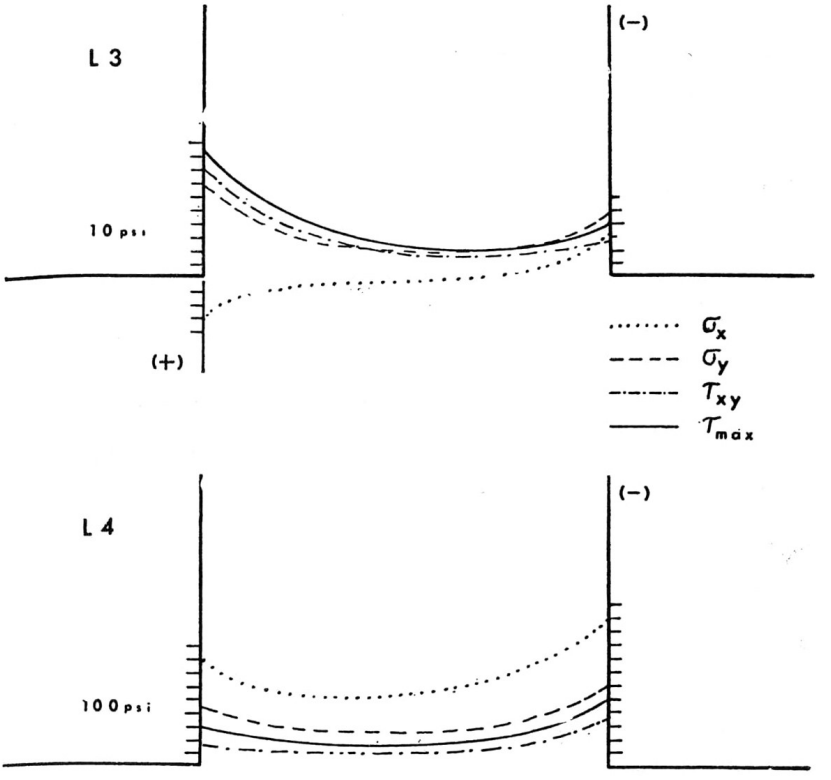


**Figure 6. Distribution of stresses at the base of the shear block at the incipient yield.**

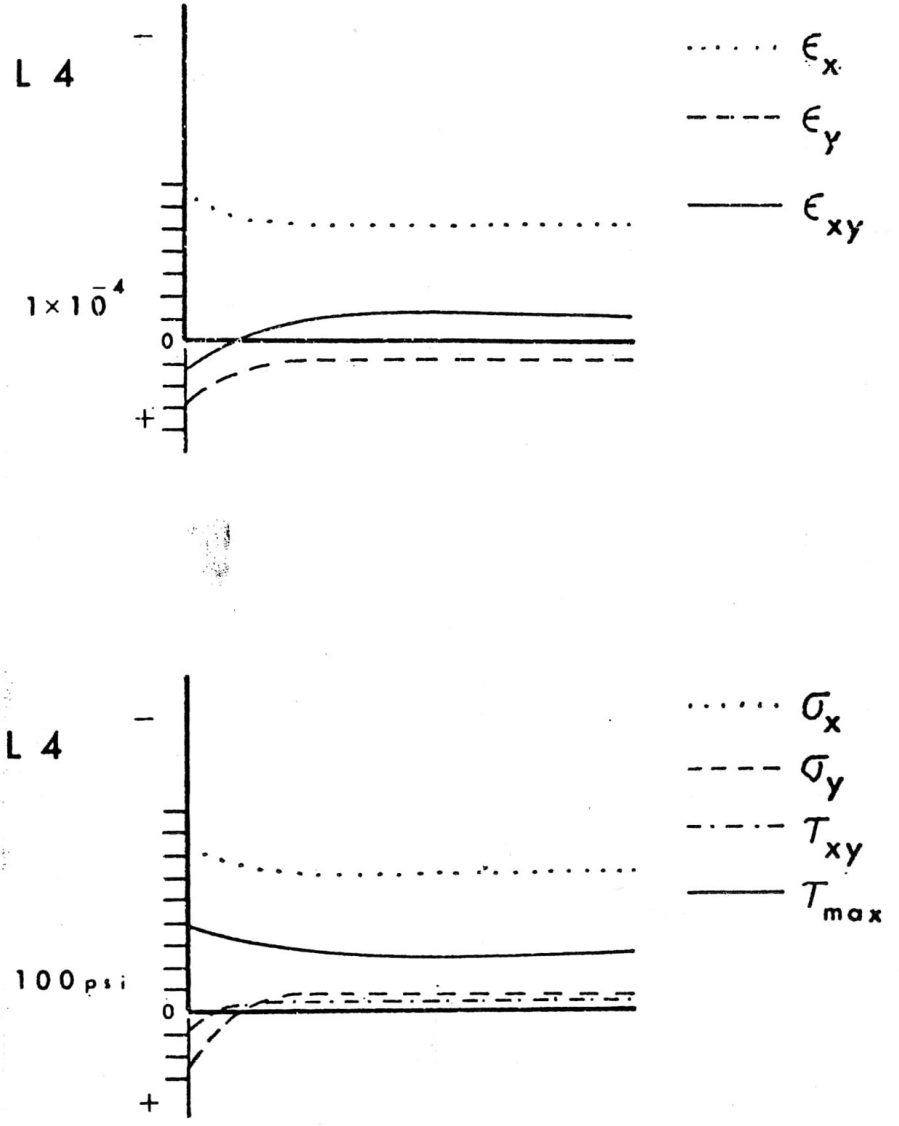


**Figure 7. Distribution of strains and stresses along discontinuity D3 at the incipient yield.**

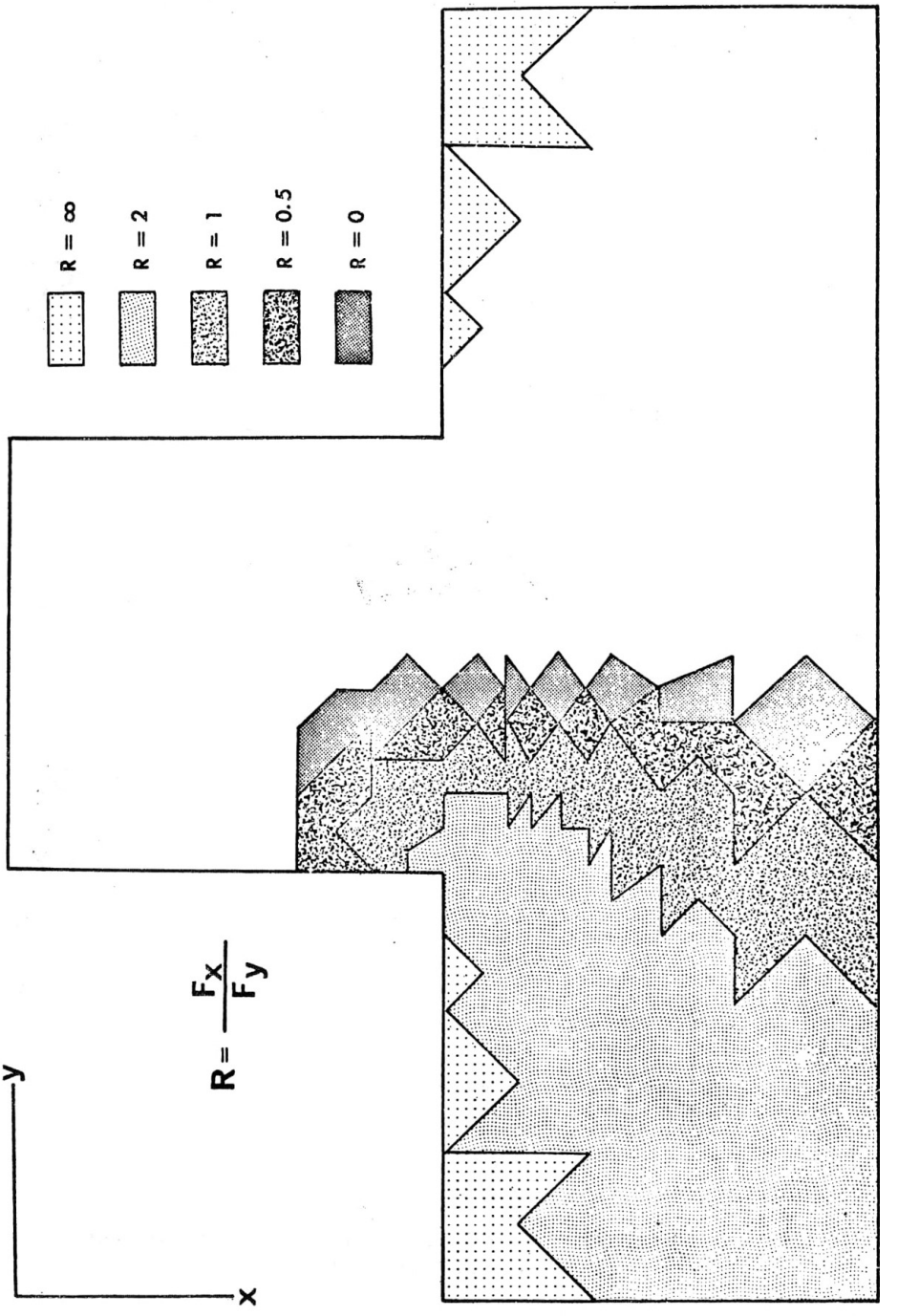


**Figure 8. Progressive development of tensile zone in the shear block.**

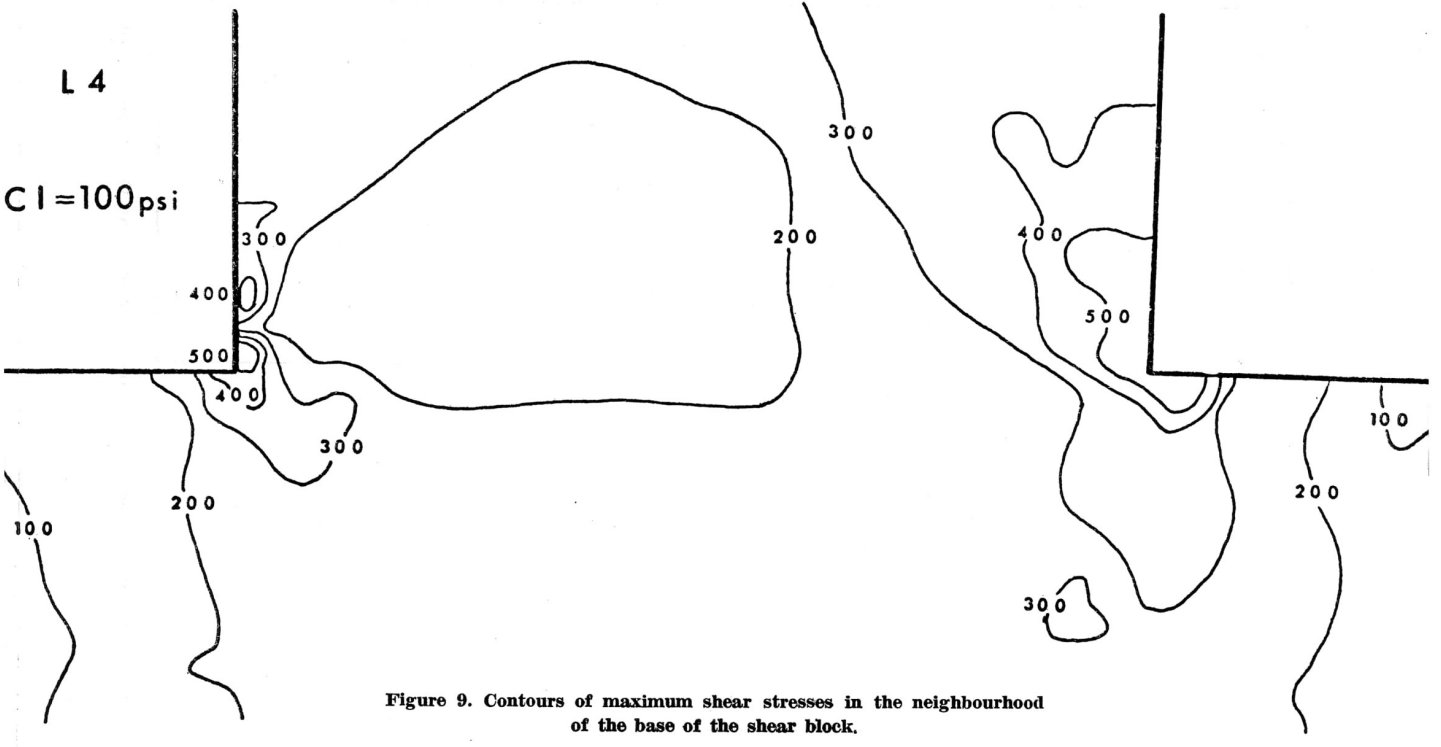


**Figure 9. Contours of maximum shear stresses in the neighbourhood of the base of the shear block.**

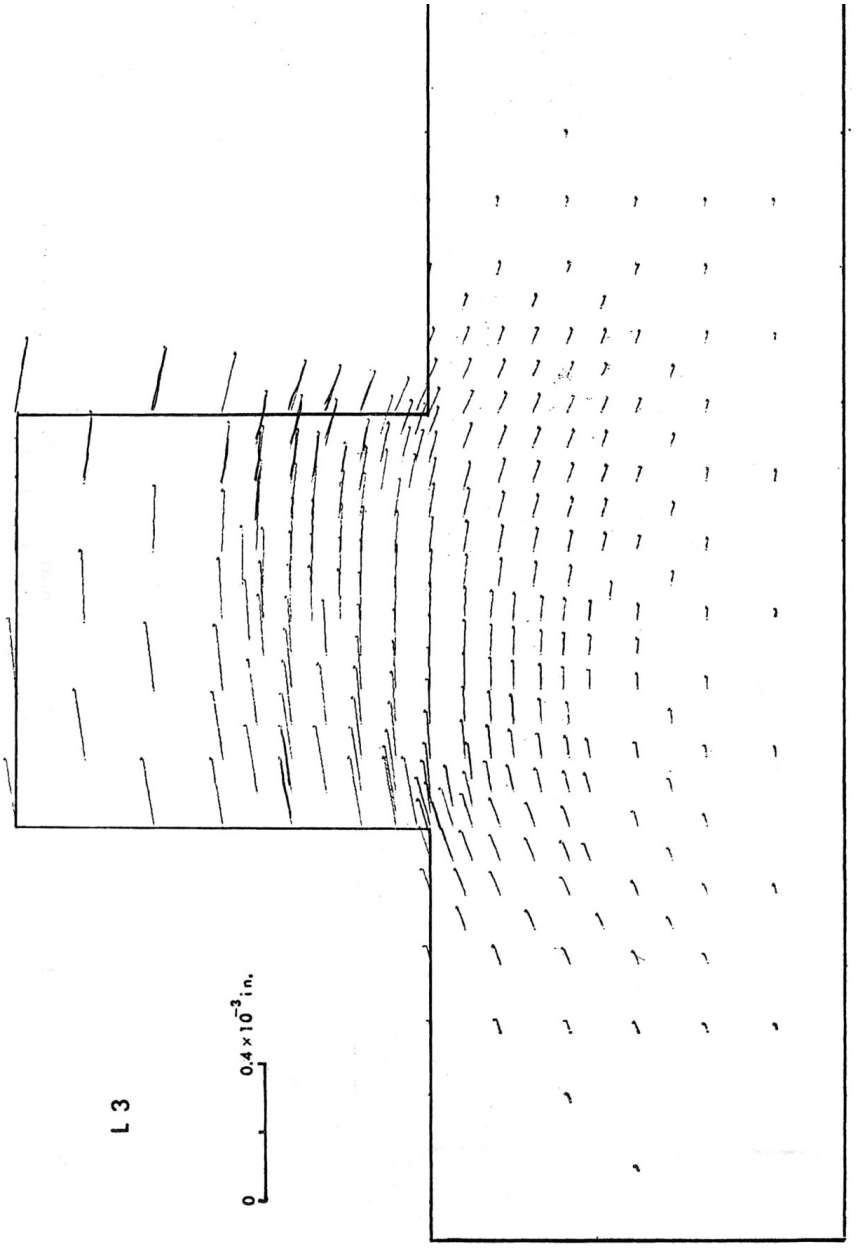


**Figure 10. Displacement field in the shear block at the incipient yield.**

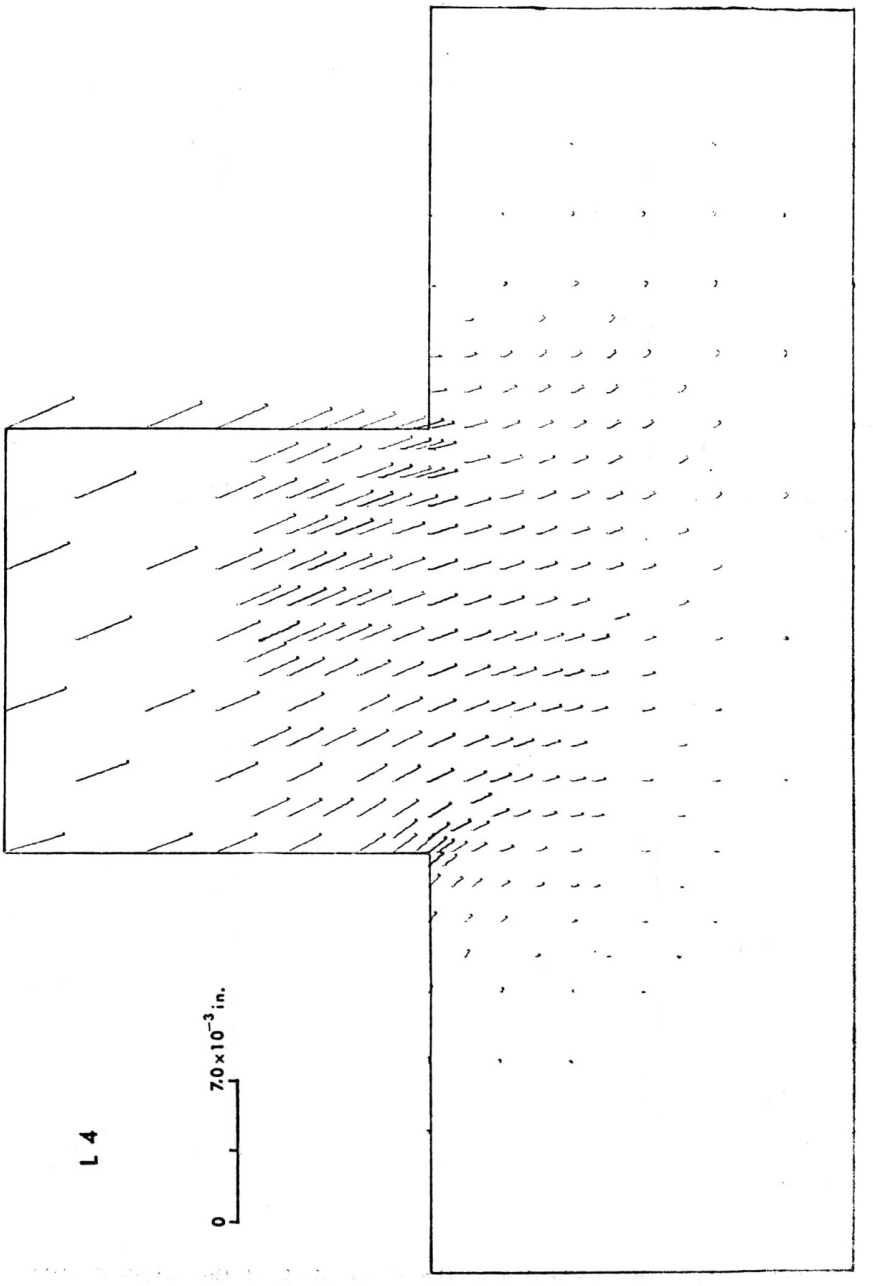


**Figure 11. Displacement field in the shear block at the incipient yield.**

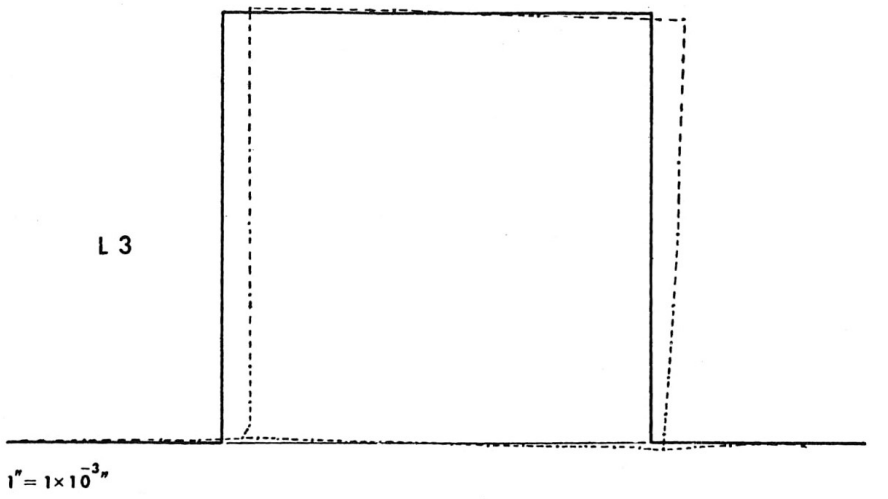


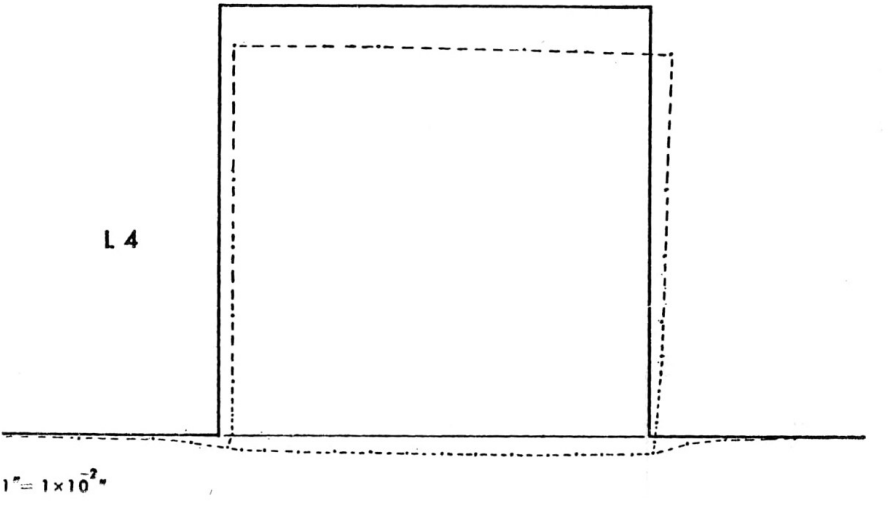


**Figure 12. External distortion of the shear block at the incipient yield.**

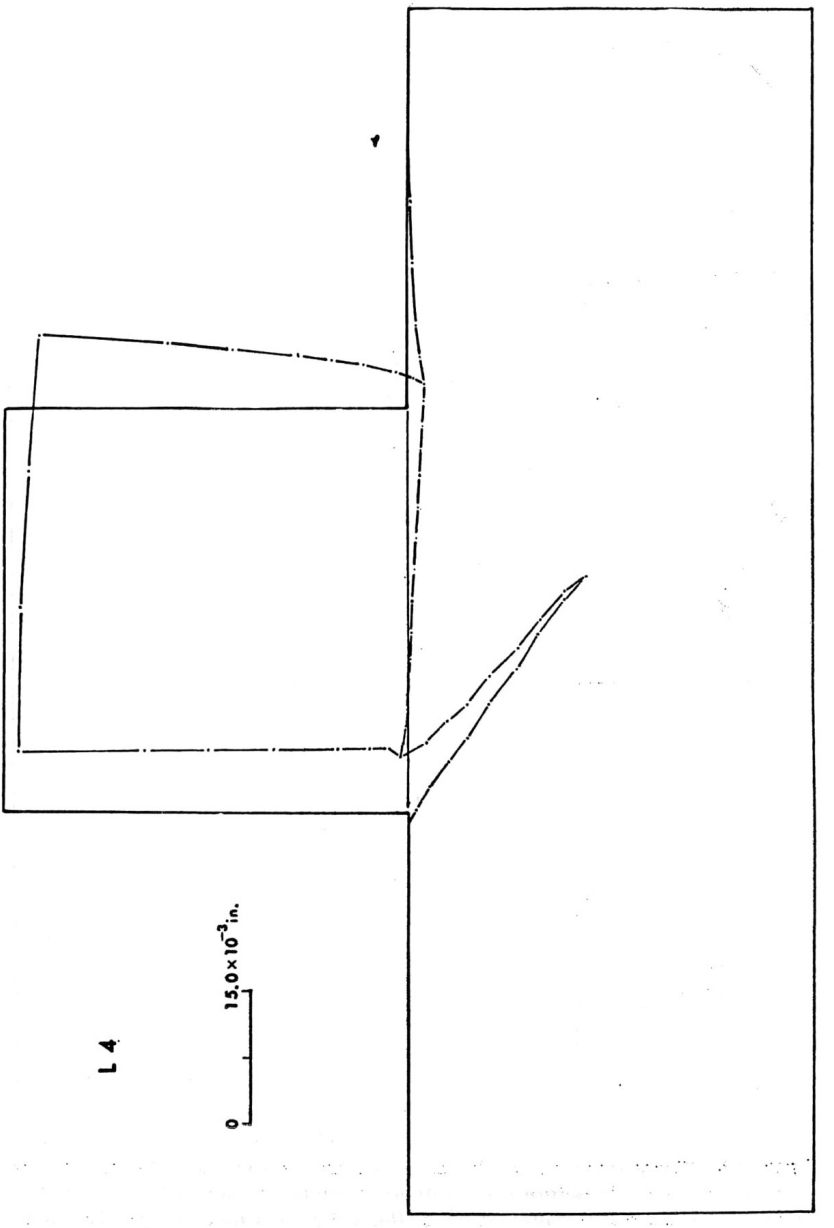


**Figure 13. Complete opening of D3 and external distortion of the shear block.**

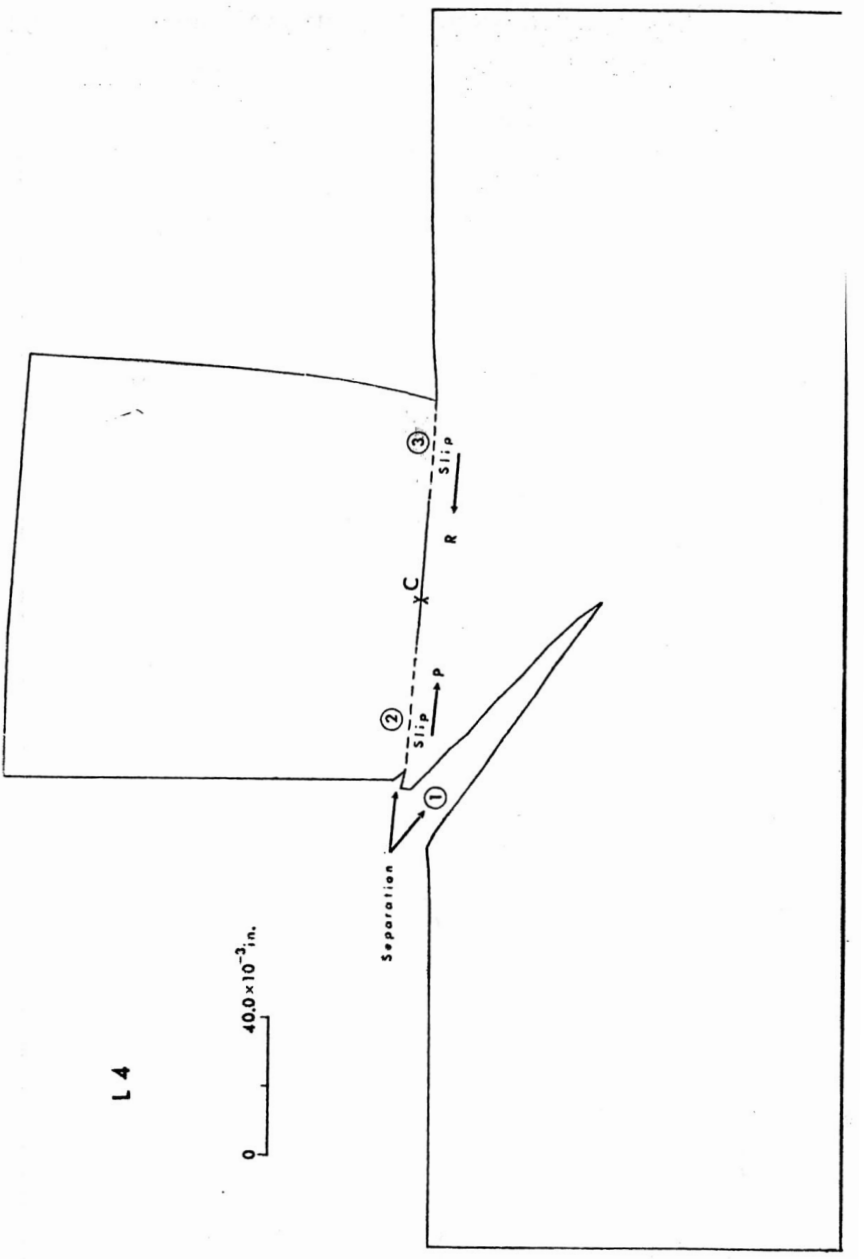


**Figure 14. Three consecutive stages of failure of the shear block (Arrows refer to direction of fracture propagation; P implies "progressive failure"; R implies "retrogressive failure"; C is the point at which progressive and retrogressive failure surfaces meet.**

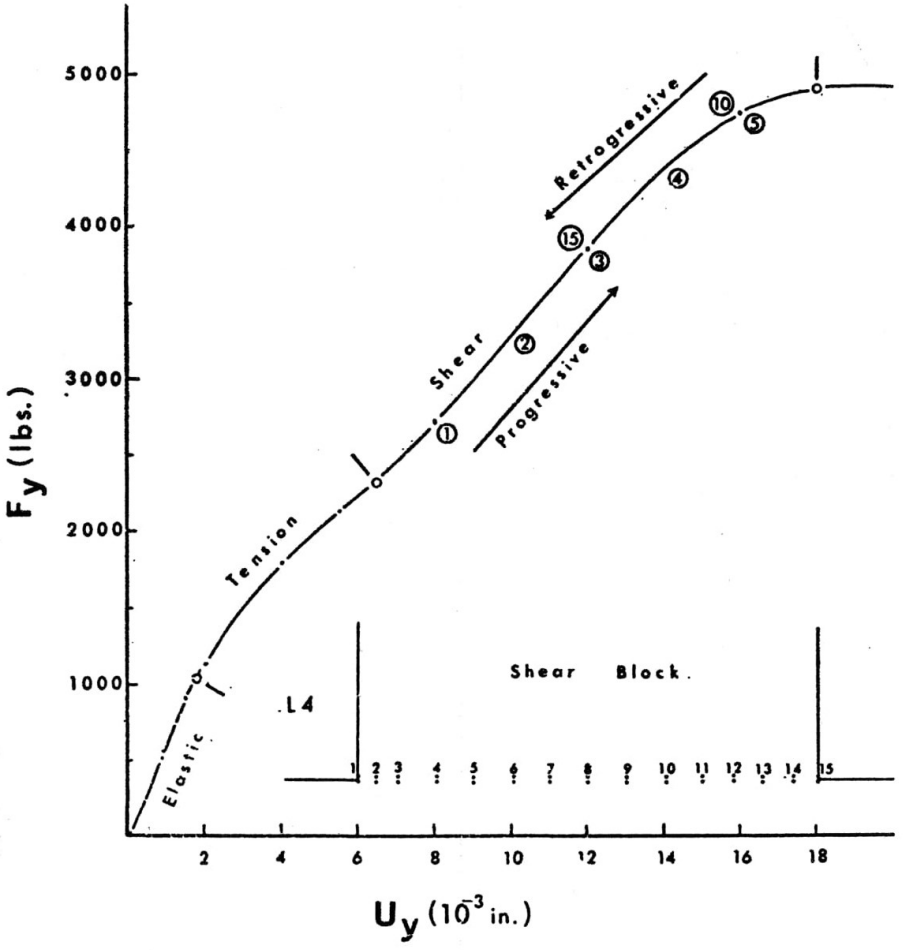


**Figure 15. "Progressive" and "Retrogressive" failure series**

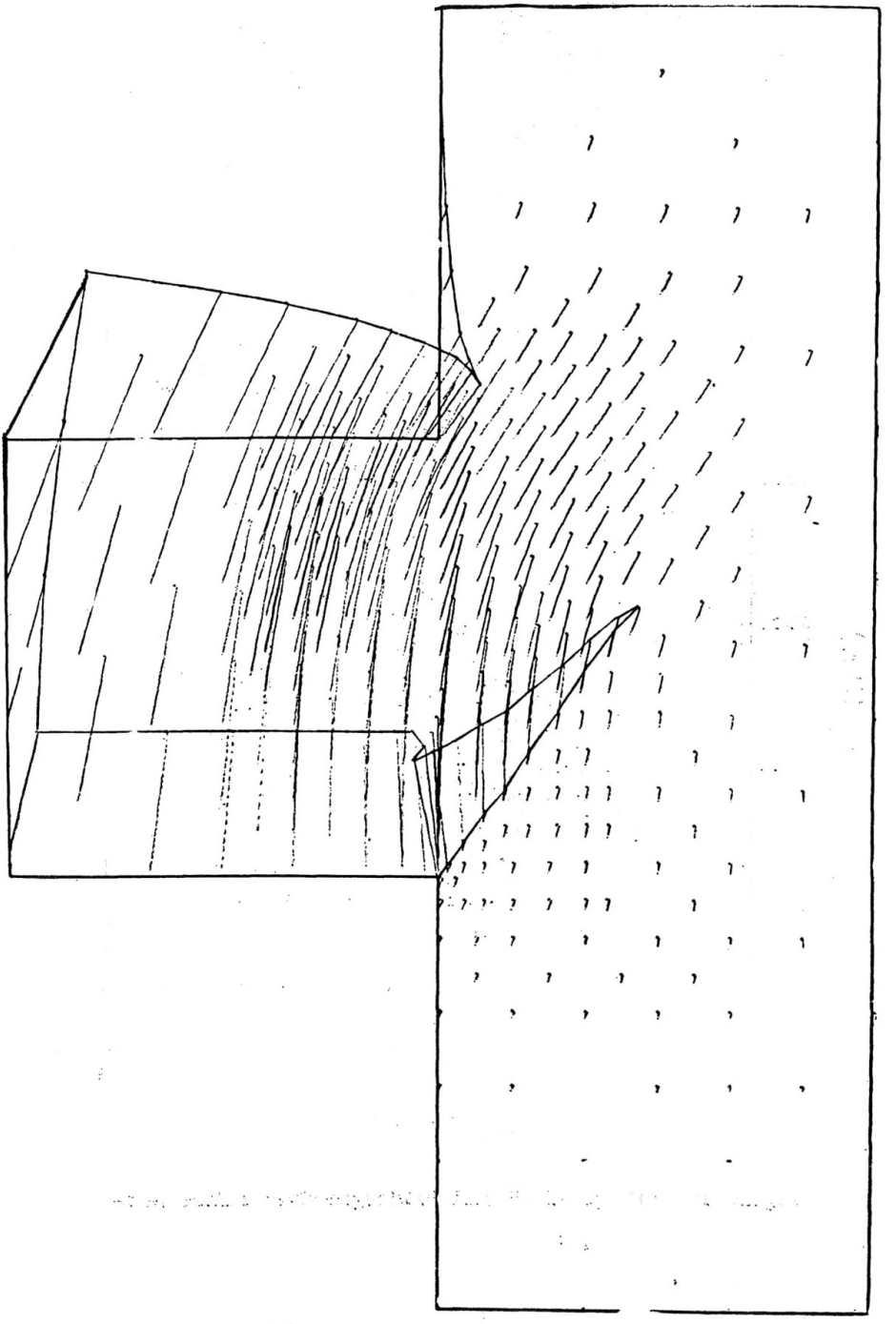

**Figure 16. Displacement field associated with "Progressive" and "Retrogressive" failure series (Complete opening of D3)**

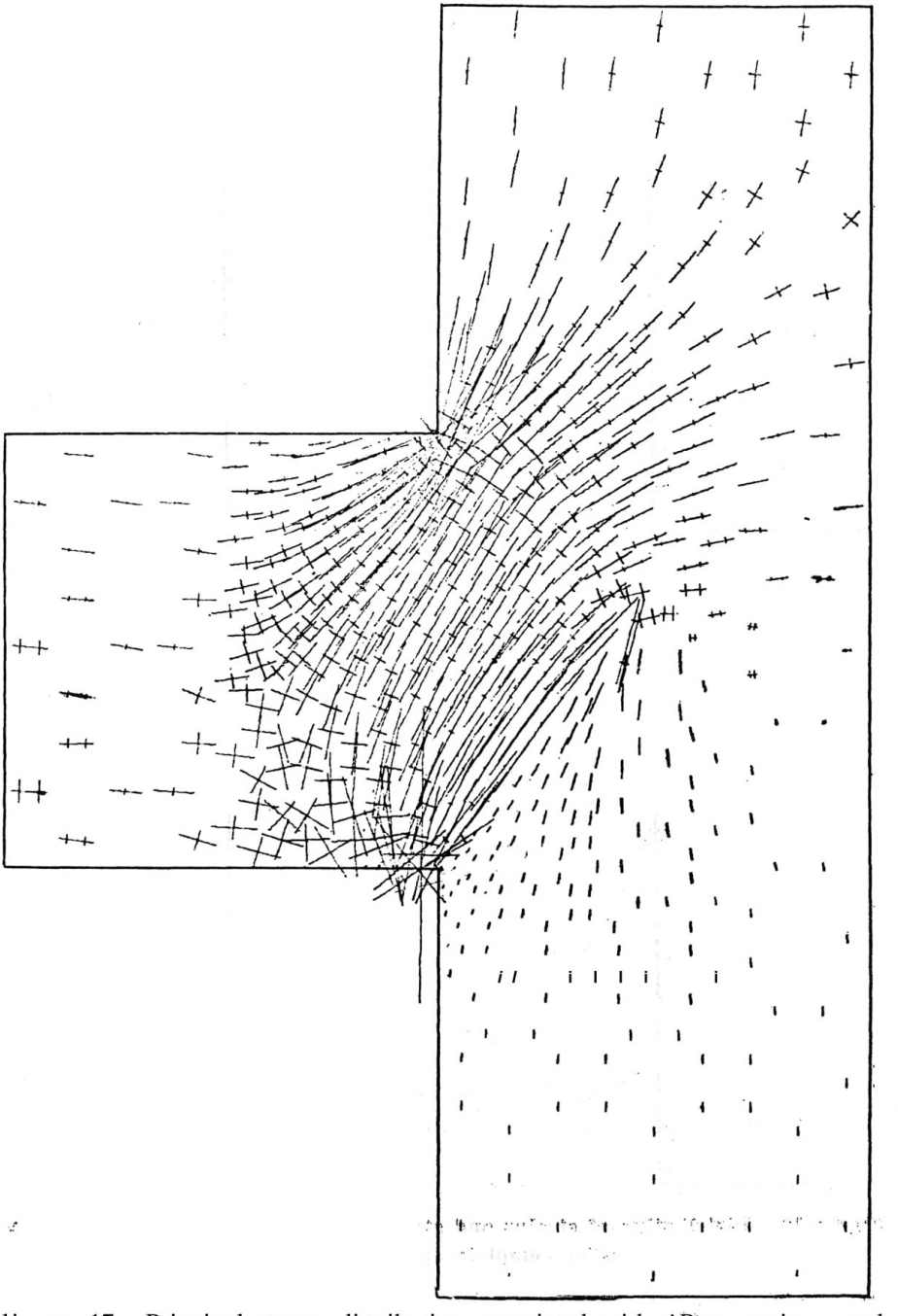

ligure 17. Principal stress distribution associated with ^Progressive and "Retrogressive'* failure series (Complete opening of D3)»

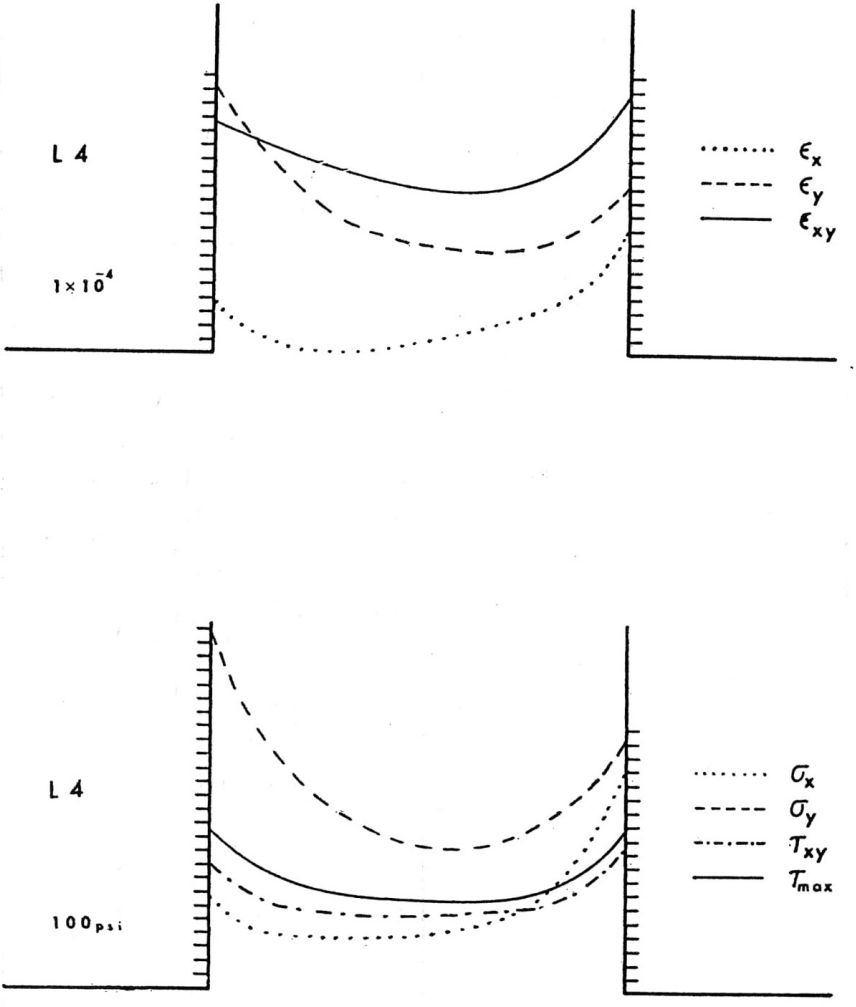


**Figure 18. Distribution of strains and stresses at the base of the shear block after complete opening of D3.**

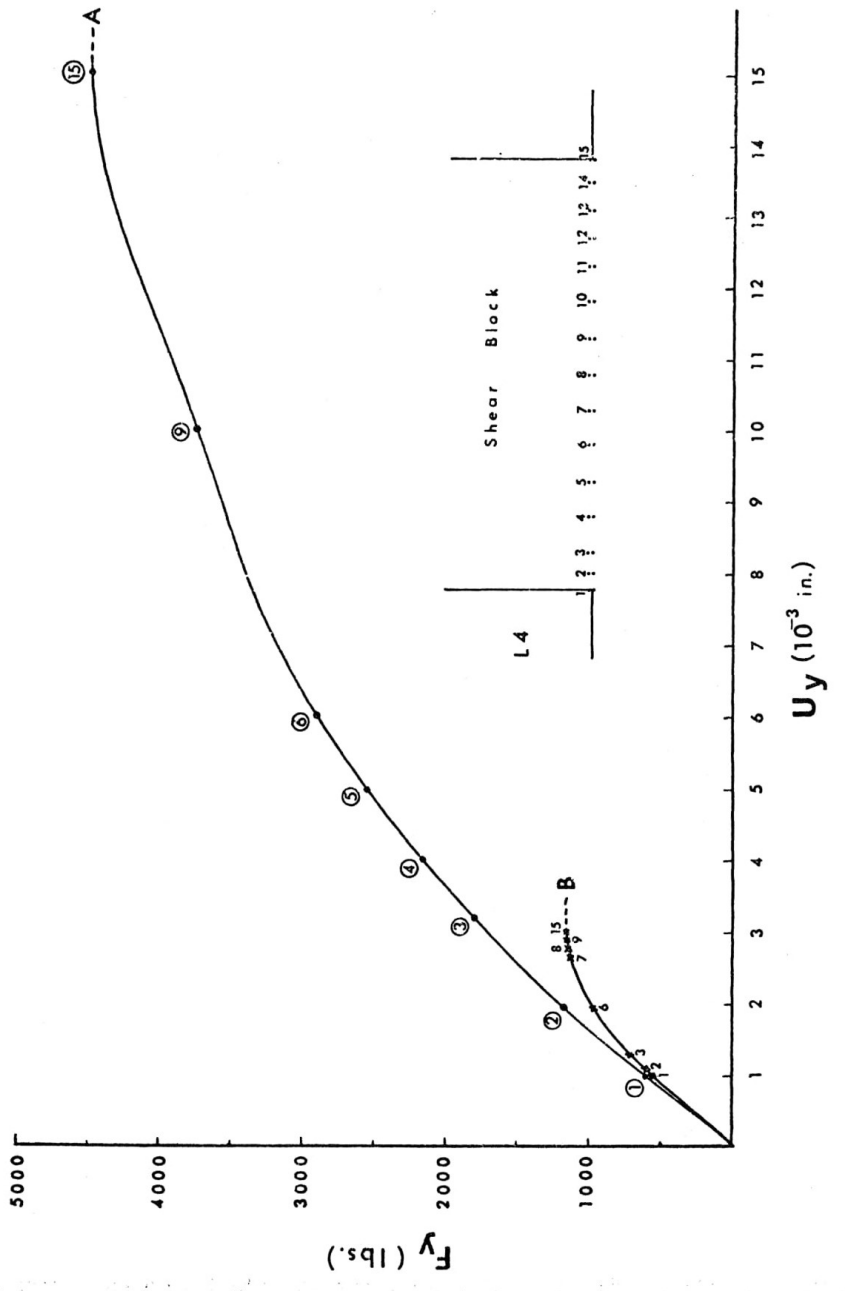


**Figure 19. Force-Displacement relationships for progressive failure: A, First series; B, Second series of computer experiments.**

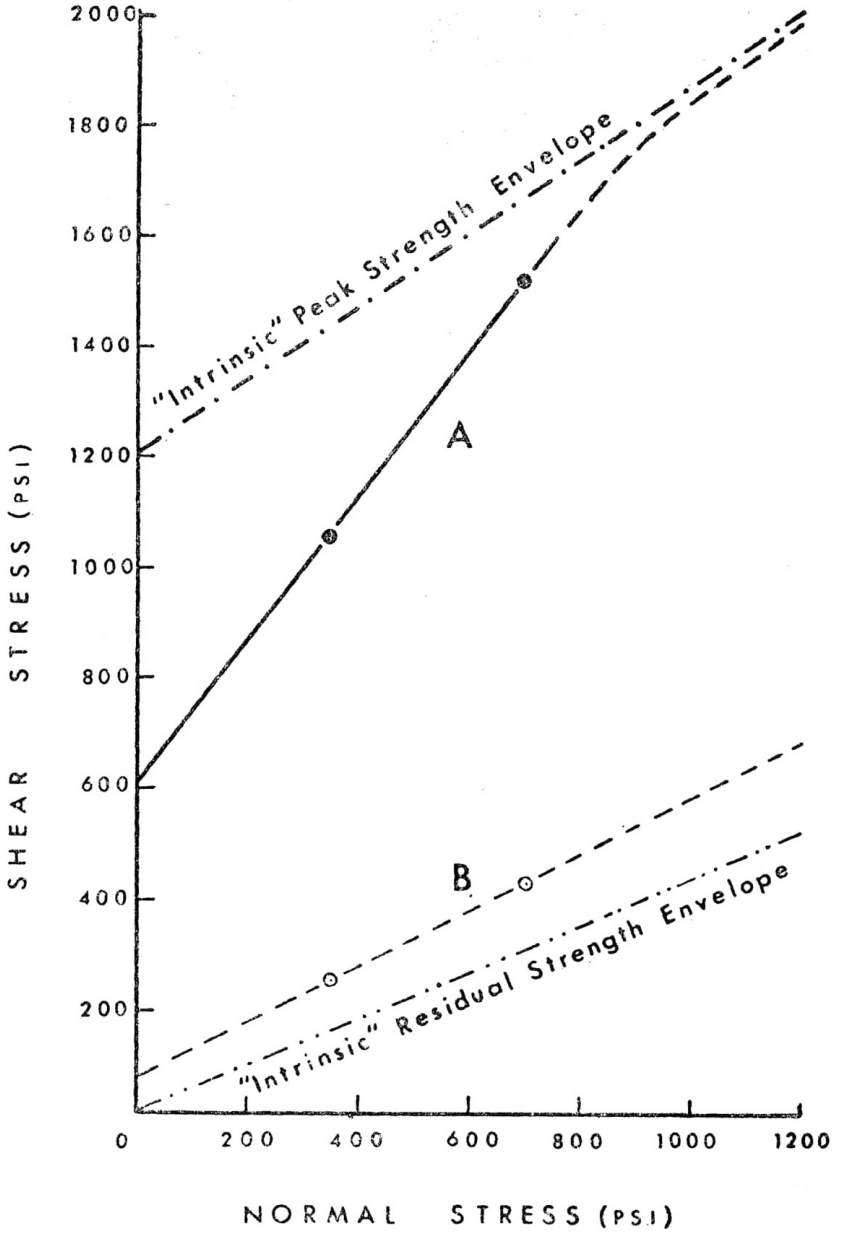


**Figure 20. "Predicted" and "Intrinsic" shear strength failure envelopes: A, predicted on the basis of peak strength retainment in "failed" region; B, predicted on the basis of residual strengths for "failed" region.**

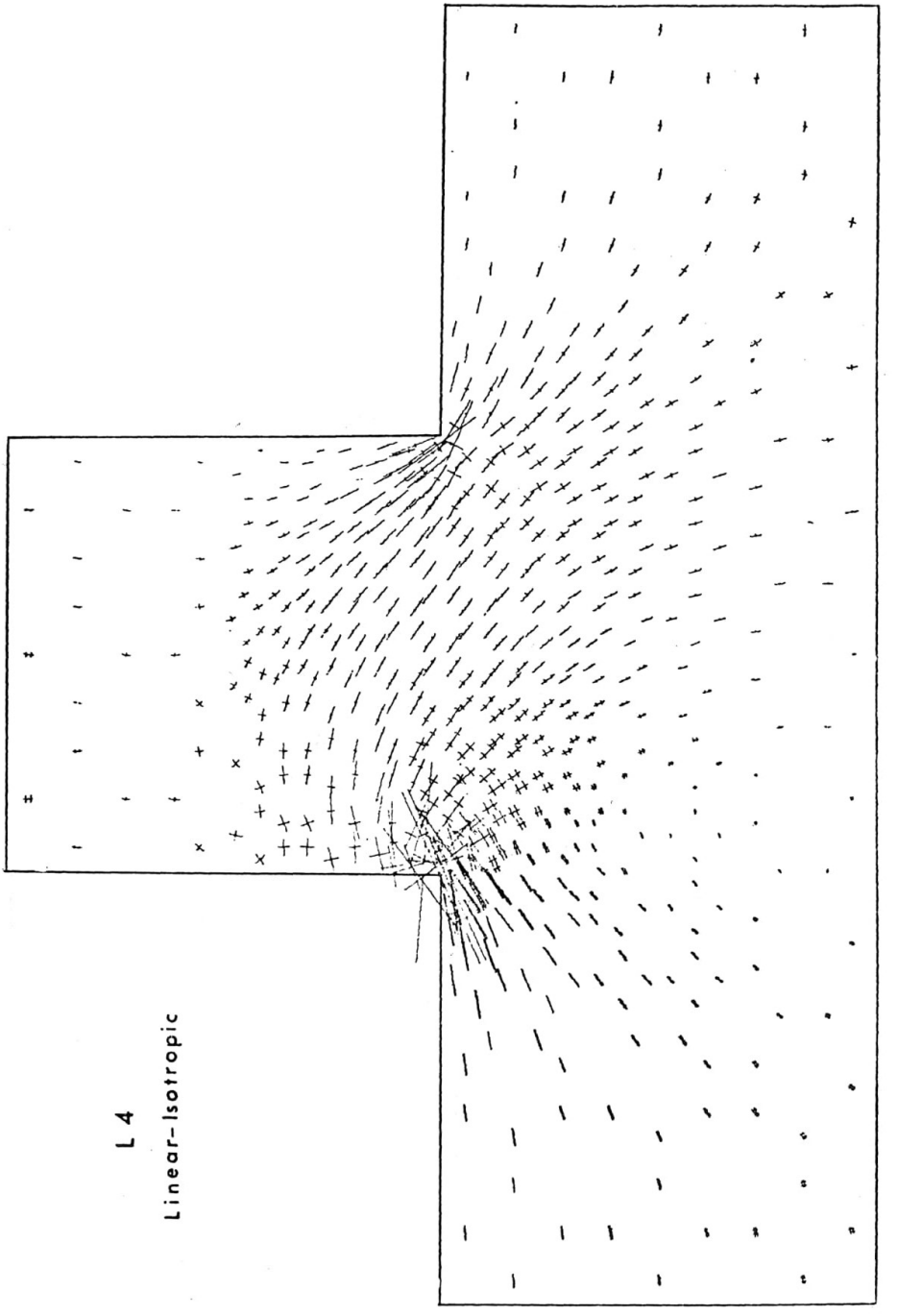


**Figure 21. Distribution of principal stress in the plastic stage of the shear block.**

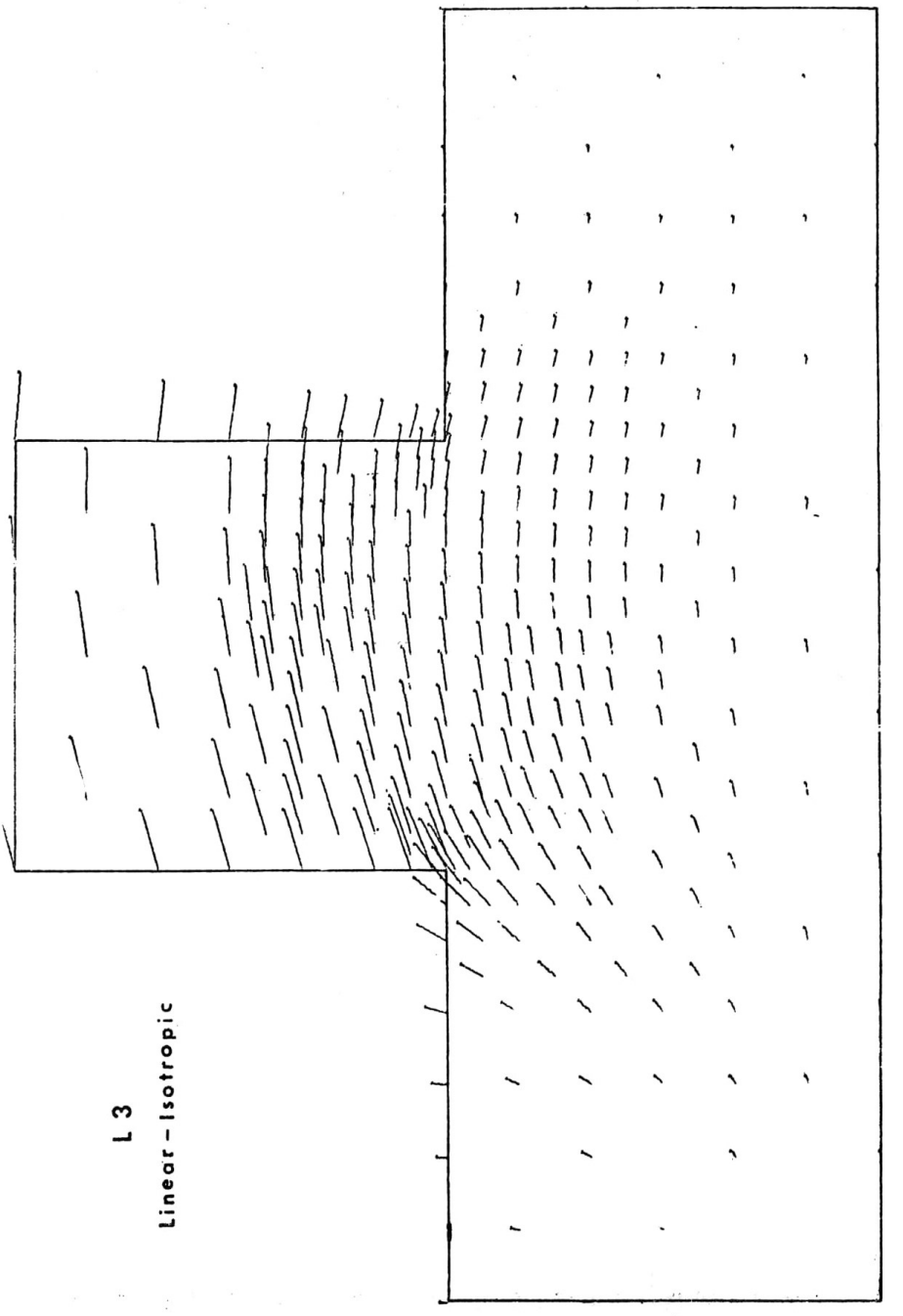


**Figure 22. Plastic displacement field in the shear block.**

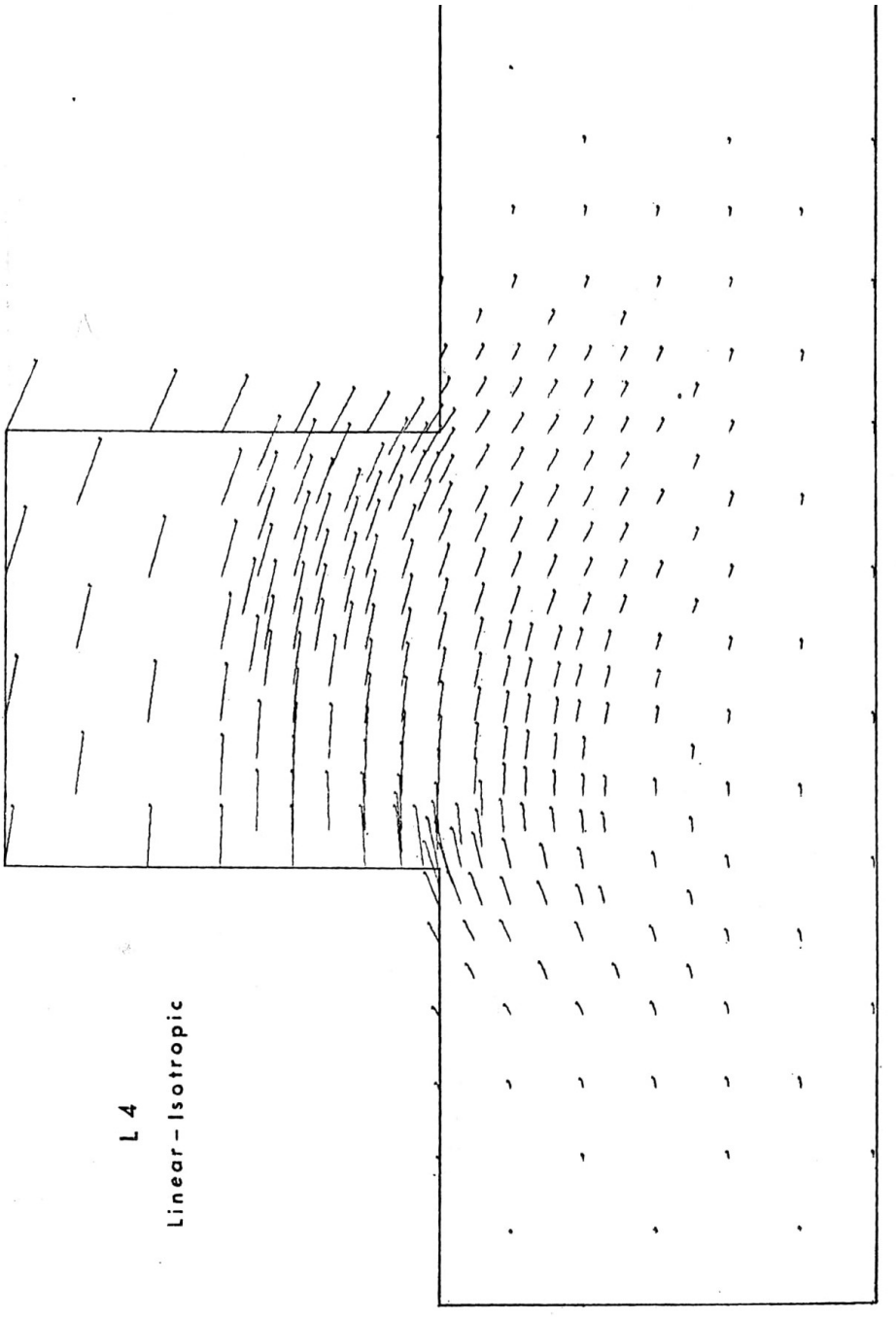


**Figure 23. Plastic displacement field in the shear block.**

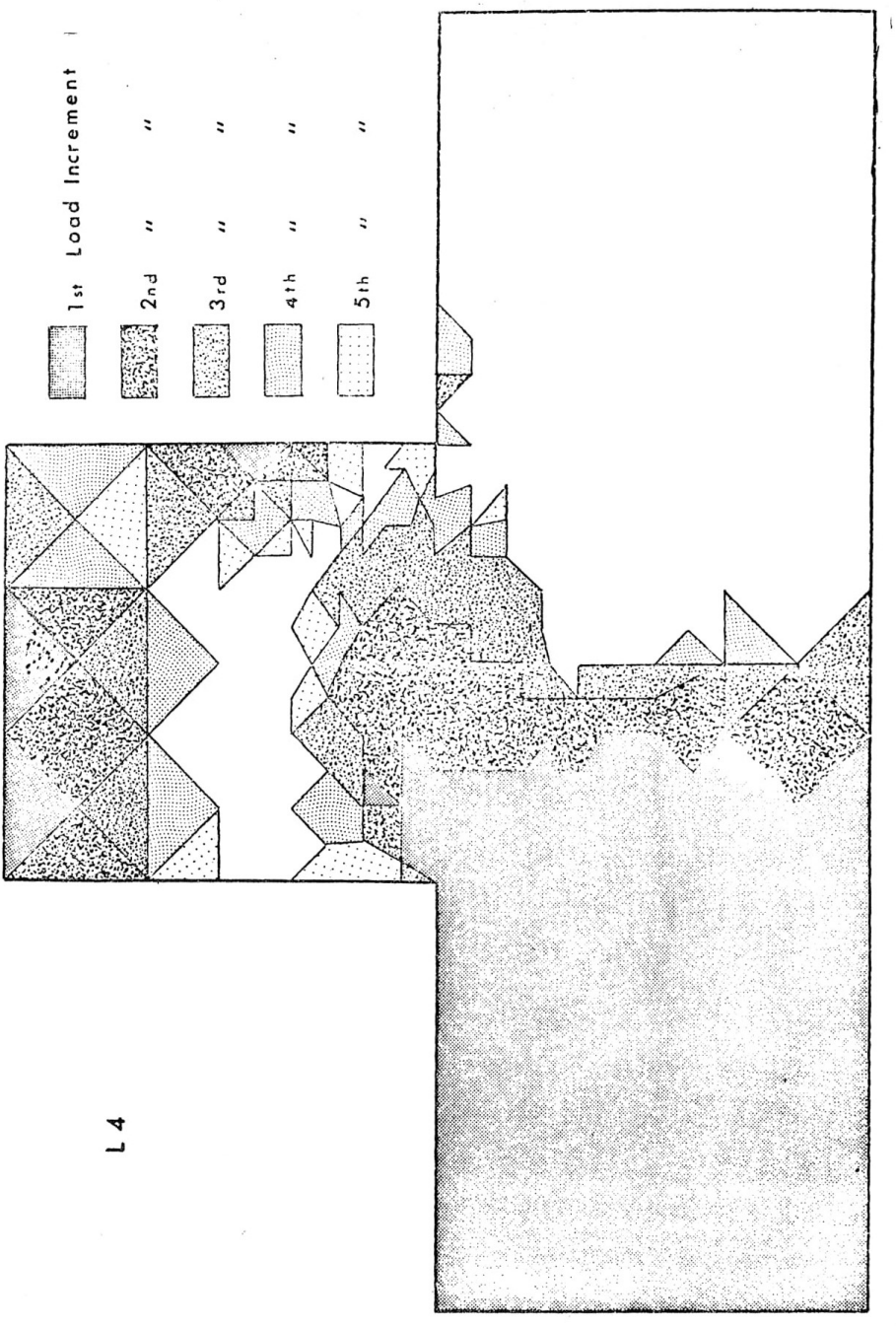


**Figure 24. Progression of the plastic yield zones in the shear block.**